Hierarchical chirality observed from chiral supramolecular assembling of racemic and enantiopure helicene derivatives on silica nanohelix surfaces

Nanami Hano, Nicolas Zigon, Balamurugan Kuppan, Ludmilla Sturm, Nicolas Vanthuyne, Emilie Pouget, Sylvain Nlate, Harald Bock, Fabien Durola, Narcis Avarvari, et al.

Hierarchical chirality observed from chiral supramolecular assembling of racemic and enantiopure helicene derivatives on silica nanohelix surfaces

publié le 18 décembre 2024 dans Nanoscale : *Nanoscale, 2025,17, 5081-5089*

Nanami Hano, Nicolas Zigon, Balamurugan Kuppan, Ludmilla Sturm, Nicolas Vanthuyne, Emilie Pouget, Sylvain Nlate, Harald Bock, Fabien Durola, Narcis Avarvari and Reiko Oda

Cast films of racemic helicene derivatives adsorbed onto the surface of nanometric silica helices with controlled handedness exhibited distinct CD signals, whereas no CD signal was observed in the absence of silica nanohelices. These CD signals originate from the helical supramolecular assemblies formed by the racemic mixture of helicenes, with no evidence of enantiospecific adsorption. Interestingly, when enantiomerically pure forms of these helicenes were drop-cast onto the silica helices, different CD spectra were observed depending on the combination of the helicenes' handedness with that of the silica nanohelices. In all cases, the sign of the CD signals was determined by the handedness of the silica helices, with positive signals for right-handed helices and negative signals for left-handed helices. Furthermore, the wavelength of the CD signal maxima is dictated by the combination of the handedness of both the helicene and silica helix and shifts from 250 to 340 nm when they have matching handedness.

Introduction

Carbohelicenes, which are composed of multiple helically connected aromatic rings, are known for their strong optical rotation and pronounced circular dichroism due to their unique helical structure. Numerous studies have reported the synthesis of carbohelicenes exhibiting these strong chiroptical signatures.[1–5] A variety of novel materials have been developed based on helicenes, including liquid crystals, nonlinear optical materials, and Langmuir–Blodgett films.[6,7] Considerable research has focused on carbohelicene derivatives featuring various functional groups, such as alkoxy,[8–10] carboxyl,[11–13] and amino groups.[14–16] Some of us have reported the synthesis of various carbohelicene derivatives from [4]helicene-carboxylic acid[17] to [6]helicene-acenones.[18] Carbohelicenes with a small number of benzene rings, namely [4]helicene and [5]helicene, are known to racemize easily at room temperature, making it challenging to evaluate their optical properties and structures.[19]

We previously reported the preparation of silica nanohelices using organic nanohelices as templates, formed by the selfassembly of a cationic gemini surfactant with a tartrate counterion.[20] The induction of chiroptical signals in achiral molecules was observed by replacing tartrate with achiral species, such as anionic polyaromatic chromophores,[21] anthracene carboxylate,[22] and dihydroxy-naphthalene[23] within silica-coated organic nanohelices. We also reported that the adsorption of achiral materials, such as perovskites,[24] gold nanoparticles[25] and various achiral dyes,[26–28] onto the surface of silica nanohelices produces a similar effect.

Extensive research has been conducted on the adsorption of amino acids and peptides on solid surfaces, revealing that the stereochemical configuration of diastereoisomers significantly affects their adsorption properties.[29,30] In diastereospecific adsorption on solid surfaces, the adsorption strength and position vary among isomers, and a specific diastereoisomer may be preferentially adsorbed.[31–33] This phenomenon has been utilized to enhance the accuracy of molecular recognition and fractionation, playing a crucial role in understanding the influence of surface chemistry on adsorption behavior. Moreover, this specific adsorption behavior holds potential applications in asymmetric synthesis and the control of catalytic reactions.

In this paper, we demonstrate that racemic helicene derivatives adsorbed onto the surfaces of silica nanohelices exhibit intriguing chiroptical signals, despite the significant difference in the scale between the two chiral structures: the silica nanohelices measure approximately 100 nm, while the helicene derivatives are at the molecular scale with a radius of about 1 nm.

Experimental

Materials

N,N′-Dihexadecyl-N,N,N′,N′-tetramethylethylene diammonium with D- or L-tartrate (gemini surfactant with D- or L-tartrate) was synthesized by a previously reported procedure.[20] Ethanol (96.9–97.2%), N,N,N′,N′-tetramethylethylene, 1-bromohexadecane, silver acetate, D-(−)-tartaric acid, L-(+)-tartaric acid, tetraethyl orthosilicate (TEOS) and (3-aminopropyl) triethoxysilane (APTES) were purchased from Sigma-Aldrich (Darmstadt, Germany). [4]helicene carboxylic acid (T1C)[34,35] was synthesized according to reported procedures; [5]helicene tetracarboxylic acid (P4C) and [6]helicene tetracarboxylic acid (H4C) (Fig. 1) were synthesized following an established procedure based on the Perkin strategy,[36] while [6]helicene carboxylic acid (H1C) was prepared through a slightly modified procedure described hereafter. In this study, the P-type (right-handed) and M-type (left-handed) [6]helicene carboxylic acids are abbreviated as P-H1C and M-H1C, respectively, and racemic mixtures of helicenes were prefixed with rac- (rac-T1C, rac-H1C, rac-P4C and rac-H4C, respectively).

Methyl (E/Z)-[4]helicene-4-vinylbenzoate. [4]Helicene-2-methyltriphenylphosphonium bromide (0.60 g, 1.03 mmol, 1 equiv.) was suspended in 20 mL of dry THF under an argon atmosphere. The mixture was cooled down to −78 °C and nBuLi (0.71 mL, 1.6 M in hexane, 1.13 mmol, 1.1 equiv.) was added dropwise. After 30 min at −78 °C, it was warmed to room temperature and stirred for one hour. The mixture was cooled down again to −78 °C and methyl 4-formylbenzoate was added (0.177 g, 1.08 mmol, 1.05 equiv.). The mixture was stirred for 10 min at −78 °C, then warmed to room temperature and left at RT overnight. After filtration on Celite and concentration under vacuum, column chromatography (SiO_2, CH_2Cl_2 : PE = 4 : 6 to 6 : 4) yielded the target compound as a yellow solid (0.37 g, 92%, mixture of Z/E isomers). ^{1}H NMR (300 MHz, $CDCl_3$): δ (ppm) 9.20 (s, 0.4 H), 9.17 (s, 0.2H), 8.98 (s, 0.6H), 8.46 (d, J = 8.6 Hz, 0.6 H), 8.15–7.65 (m, 9.8 H), 7.63–7.47 (m, 3H), 7.41–7.26 (m, 1.35H), 7.02 (d, J = 12.1 Hz, 0.6H), 6.81 (d, J = 12.1 Hz, 0.6H), 3.99 (s, 0.9H), 3.93 (s, 2H) (Fig. S7†). ^{13}C NMR (75 MHz, $CDCl_3$): δ (ppm) 167.04, 166.99, 142.47, 142.00, 134.88, 134.69, 133.73, 133.53, 133.50, 133.05, 132.79, 131.96, 131.51, 131.34, 130.72, 130.48, 130.42, 130.22, 129.95, 129.91, 129.37, 129.19, 129.07, 128.84, 128.78, 128.63, 128.55, 128.08, 127.88, 127.85, 127.82, 127.74, 127.57, 127.52, 127.37, 127.28, 127.25, 126.98, 126.90, 126.56, 126.52, 126.46, 126.29, 126.11, 125.99, 123.31, 77.58, 77.16, 76.74. R_f (SiO_2, CH_2Cl_2 : PE 4 : 6) = 0.33. MS (MALDI) m/z = 387.9, theor. calc. 388.1 ($M^{\bullet+}$) (Fig. S8 and S9†).

Methyl [6]helicene-15-carboxylate. Methyl [4]helicene-4-vinylbenzoate (0.37 g, 0.95 mmol, 1 equiv.) was dissolved in 700 mL of degassed toluene in a photoreactor. Iodine (0.27 g, 1.05 mmol, 1.1 equiv.) and propylene oxide (3.5 mL) were added and the mixture was irradiated with an immersion lamp (150 W) for 16 hours. After evaporation of the solvent, column chromatography (SiO_2, PE:CH_2Cl_2 6 : 4 to 2 : 8) was performed. The compound was dissolved in a minimal amount of CH_2Cl_2 and precipitated with PE. Methyl [6]helicene-15-carboxylate was obtained as a yellow solid (0.19 g, 52%). The resolution of the enantiomers was performed by chiral HPLC (see the ESI). ^{1}H NMR (300 MHz, $CDCl_3$): δ (ppm) 8.38 (s, 1H), 8.08–7.77 (m, 11 H), 7.53 (d, J = 8.5 Hz, 1H), 7.18 (d.d., J = 7.2 Hz; 7.1 Hz, 1H), 6.65 (d.d., J = 8.2 Hz; 7.2 Hz, 1H), 3.59 (s, 3H) (Fig. S10†). ^{13}C NMR (75 MHz, $CDCl_3$): δ (ppm) 166.81, 134.35, 133.43, 132.55, 131.69, 131.53, 130.87, 130.24, 129.51, 129.04, 128.97, 128.53, 127.97, 127.93, 127.83, 127.76, 127.62, 127.51, 127.37, 127.24, 127.05, 126.54, 125.91, 125.82, 125.25, 124.75, 124.09, 51.50. R_f (SiO_2, CH_2Cl_2 : PE 4 : 6) = 0.3 (Fig. S11 and S12†).

[6]Helicene-11-carboxylic acid (H1C). Methyl [6]helicene-15-carboxylate (0.19 g, 0.49 mmol, 1 equiv.) and MeONa (7.96 g, 147 mmol, 300 equiv.) were dissolved in 100 mL of MeOH and 10 mL of H_2O. After 7 days of reflux, the solvent was evaporated to a volume of approx. 50 mL. H_2O (150 mL) was added followed by HCl 10% until pH = 2 (ca. 150 mL). After filtration, the residue was washed with cold EtOH and dried under vacuum to yield H1C as a white solid (0.18 g, quant.). ^{1}H NMR (300 MHz, DMSO-d_6): δ (ppm) 8.25–7.96 (m, 11H), 7.89 (d, J = 8.0 Hz, 1 H), 7.72 (d.d., J = 8.3 Hz; 1.6 Hz, 1 H), 7.39 (d, J = 8.7 Hz, 1 H), 7.23 (d.d., J = 7.3 Hz; 7.3 Hz, 1 H), 6.66 (d.d., J = 8.2 Hz; 8.0 Hz, 1 H) (Fig. S13†). HR (MALDI) m/z = 372.1154, theor. calc. 372.1145 ($M^{\bullet+}$).

Preparation of aminated silica nanohelices

The preparation of silica nanohelices[20] and the amination of their surface were performed through the following four steps (Fig. 2). Formation of organic nanohelices. Organic nanohelices were prepared by the self-assembly of a gemini surfactant with either L- or D-tartrate in water. The gemini surfactant with L-tartrate self-assembles to P-type (right-handed) helices, whereas with D-tartrate, they form M-type (left-handed) helices (Fig. S1a and b†). A 3.57 mg sample of the surfactant was dispersed in 5 mL of water using ultrasonic irradiation and then solubilized by heating at 60 °C for 10 min in a water bath. The solution was cooled down and incubated at 20 °C for 4 days.

Preparation of silica-coated nanohelices (hybrid nanohelices). Separately, 0.5 mL of TEOS was mixed with 10 mL of an aqueous solution of L- or D-tartaric acid (0.1 mM) and stirred at 20 °C for 7 hours. Then, 5 mL of this acid solution was added to the organic nanohelix dispersion and allowed to react at 20 °C for 20 hours, during which polycondensation of TEOS occurred. Silica-coated organic nanohelices (hybrid nanohelices) were collected by centrifugation and washed with cold water.

Removal of organic components. The organic components inside the hybrid structure were removed by washing with ethanol (3 times, 60 °C, 10 min) and isopropanol (3 times, 60 °C, 10 min). After thorough washing, the silica nanohelices were dispersed in ethanol.

Amination of silica nanohelices. Finally, 1.0 g of APTES was added to 5 mL of silica nanohelix dispersion (0.5 mg mL^{-1}) and stirred at 80 °C for 24 hours in an oil bath. TEM images of the silica nanohelices after amination showed that the helical shape was preserved (Fig. S1c and d†). The aminated silica nanohelices were then washed with ethanol 3 times to obtain the final product. After surface treatment, aminated silica nanohelices (ASNHs) showed –NH stretching vibrations originating from amino groups around 1560 cm^{-1}. In addition, it was observed that the CH stretching vibration derived from the alkyl group increased around 2980 cm^{-1} and the OH stretching vibration decreased around 3300 cm^{-1}. These results suggest that the silanol groups on the silica nanohelix surface are reduced and the amino groups are modified (Fig. S2†). Hereafter, right- and left-handed aminated silica helices (ASNHs) are denoted as P-S and M-S, respectively.

Preparation of drop-cast films with silica nanohelices and various helicene derivatives

The procedures for preparing drop-cast films of aminated silica nanohelices and helicene-grafted silica nanohelices are illustrated in Fig. S3.† For the aminated silica nanohelices, 50 µL of an ethanol dispersion (1 mg mL^{-1}) was drop-cast onto a quartz glass substrate (1 cm × 1 cm) and dried at room temperature. In the case of helicene-grafted silica nanohelices, they were suspended in DMF, and 50 µL of the dispersion was drop-cast and dried at room temperature.

Characterization

Surface characterization. Characterization of organic components after surface modification of silica nanohelices was performed using attenuated total reflection (ATR, Everest) with Fourier transform infrared spectroscopy (ATR-FTIR, Thermo Fisher Scientific Inc., Waltham, USA). Silica nanohelix powders before and after surface modification were placed on ATR crystals (diamond) and measured in the range from 500 to 4000 cm^{-1} with a resolution of 8 cm^{-1}.

Morphological analysis. The morphology of the silica nanohelices was characterized using transmission electron microscopy (TEM, CM120, Philips, Amsterdam, Netherlands). TEM observation samples were prepared by dropping 7 µL of silica nanohelix/ethanol dispersion (0.04 µg $µL^{-1}$) onto a carbon supported copper grid and drying without staining. The observation was performed at 120 kV.

Chiroptical and UV-Vis measurements. Circular dichroism (CD) and UV-visible (UV-Vis) absorption spectra of the silica nanohelices and helicene mixtures were recorded using a CD spectropolarimeter (J-815, JASCO Corp., Tokyo, Japan) equipped with a 1 mm path length quartz cell. Diffuse reflectance circular dichroism (DRCD) and UV-Vis spectra of the drop-cast films were obtained using an integrating sphere (DRCD-575) attached to the J-815.

Circularly polarized luminescence (CPL) and fluorescence measurements. CPL and fluorescence spectra of the drop-cast films were measured using a CPL spectrophotometer (CPL-300, JASCO Corp., Tokyo, Japan). The measurements were carried out with an HT voltage of 700–750 V. Emission was detected in the wavelength range of 400–800 nm. Samples were excited using monochromatic light sources with excitation wavelengths of 295 nm (rac-T1C), 300 nm (rac-H1C) and 330 nm (rac-P4C and rac-H4C), respectively.

Results and discussion

Investigation of helicene enantiomer adsorption selectivity on silica nanohelices

To examine whether these helicenes exhibit enantioselective adsorption on right- and left-handed ASNHs (P-S or M-S), a racemic [6]helicene solution (rac-H1C or rac-H4C) was mixed with an ethanol dispersion of ASNH and stirred at 20 °C for 24 hours in a roller mixer set at approx. 30 rpm. The composition ratios of the ASNH (P-S or M-S) and helicenes (rac-H1C or rac-H4C) are summarized in Table 1. In the mixture, the final concentrations of rac-H1C and rac-H4C were 0.5 mM and 0.3 mM, respectively, with P-S or M-S concentrations set at either 1.0 mg mL^{-1} or 0.2 mg mL^{-1}. After 24 hours of mixing, centrifugation (29 500g, 20 min) was performed to separate the supernatant from the precipitate. The precipitate was then

redispersed in 0.5 mL of ethanol, and CD measurements were conducted (Fig. 3). For H1C, the majority (81%) remained in the supernatant, as confirmed by the absorption signal (Fig. S4d†). However, a weak absorption signal corresponding to a helicene was observed in the UV-Vis spectra of the precipitates (P-$S_{1.0}$@rac-H1$C_{0.5}$ and M-$S_{1.0}$@rac-H1$C_{0.5}$) (Fig. 3d), indicating that rac-H1C was partially adsorbed onto the surface of the silica nanohelices. No CD signals were detected in either the supernatant or the redispersed silica nanohelices (Fig. S4a†).
A higher percentage of rac-H4C was adsorbed onto the silica nanohelices compared to rac-H1C, with 70–76% of rac-H4C bound to the nanohelices and 24–30% remaining in the supernatant (Fig. S4e†). Positive CD signals were observed for P-$S_{1.0}$@rac-H4$C_{0.3}$ and negative CD signals for M-$S_{1.0}$@rac-H4$C_{0.3}$ from the redispersed ASNH (Fig. 3b), while no CD signals were detected in the supernatants (P-$S_{1.0}$@rac-H4$C_{0.3}$ and M-$S_{1.0}$@rac-H4$C_{0.3}$) (Fig. S4b†). The higher amount of adsorption of rac-H4C onto the ASNH compared to that of rac-H1C can be attributed to the presence of four carboxyl groups, which interact with the amino groups on the silica surface via many interaction points. When a five times lower concentration of ASNH was mixed with rac-H4C, the CD signals from the redispersed precipitates decreased (P-$S_{0.2}$@rac-H4$C_{0.3}$ and M-$S_{0.2}$@rac-H4$C_{0.3}$) (Fig. 3c). This reduction in CD signals is due to the lower available surface area of the ASNH, which decreased the amount of adsorbed rac-H4C. Absorption spectra indicated that 79–86% of rac-H4C remained in the supernatant. In all cases, no CD signals were observed in the supernatants, suggesting that the helicene molecules adsorbed onto ASNH were in a racemic form, with no enantiomeric selectivity observed during the adsorption process. The high racemization barrier for [6]helicenes (around 150 kJ mol^{-1}) makes a change of conformation upon adsorption of the molecules unlikely at a temperature of 60 °C and on the timescale of the experiment.[37]
Interestingly, when the redispersed suspensions of the ASNH with helicenes were drop-cast onto quartz glass (1 cm × 1 cm), distinct DRCD signals were observed, even for samples that did not show any CD signals in suspension (Fig. 4a and c). P-$S_{1.0}$@rac-H1$C_{0.5}$–precipitate and M-$S_{1.0}$@rac-H1$C_{0.5}$–precipitate exhibited positive and negative CD signals, respectively (Fig. 4a), while P-$S_{0.2}$@rac-H4$C_{0.3}$–precipitate and M-$S_{0.2}$@rac-H4$C_{0.3}$–precipitate also showed positive and negative CD signals (Fig. 4c). For P-$S_{1.0}$@rac-H4$C_{0.3}$–precipitate and M-$S_{1.0}$@rac-H4$C_{0.3}$–precipitate, which already exhibited CD signals in suspension, the signals from the drop-cast films were approximately 10 times stronger (Fig. 4b).
These results indicate that in all cases, helicenes were successfully adsorbed onto the silica surface. Upon drop-casting and drying the complex nanohelices with helicenes, a strong enhancement of the CD signals was observed.

Preparation of drop-cast films with ASNHs and various helicene derivatives

Drop-cast films were prepared using four different helicene derivatives along with right- and left-handed ASNHs (P-S and M-S), and their CD signals were measured. Table 2 summarizes the composition ratios of the ASNHs and helicenes. The DRCD and UV-Vis absorption spectra of these drop-cast films are shown in Fig. 5. In all the films, helicene-related absorption was observed in the 200–400 nm wavelength region, along with distinct CD signals. Note that for these spectra, first, the substrates were prepared by drop-casting and drying the suspension of ASNHs. Then the solutions of helicenes were drop-cast and dried. Therefore, differently from the films analyzed in Fig. 4, in which only helices in interaction with ASNHs are drop-cast on the substrates, the films analyzed in Fig. 5 contain excess amount of helicenes that is not adsorbed on the silica helix surface.
For rac-T1C and rac-H1C, positive and negative CD spectra were detected for P-S@rac-T or H1C and M-S@rac-T or H1C, respectively (Fig. 5a and b). In the case of rac-P4C and rac-H4C helicenes, similar CD signals were observed, where P-S@rac-P/H4C exhibited a positive CD signal at around 250 nm and a negative signal at around 350 nm, while M-S@rac-P/H4C displayed the opposite trend (Fig. 5c and d).
It is important to note that rac-T1C and rac-P4C ([4]helicene and [5]helicene) are known to racemize easily, suggesting that the helicene handedness may change upon interaction with the silica nanohelices' surface. In contrast, rac-H1C and rac-H4C ([6]helicenes) are structurally stable under ambient conditions, making their handedness less likely to change.[37] In all cases, drop-cast films of helicenes without ASNH exhibited no CD signals, indicating that the CD induction is a result of the helicene adsorption onto the silica nanohelices' surface.
When comparing the drop-cast films of rac-H1C and rac-H4C, which have different numbers of substituted carboxylic acids (Fig. 5b and d), the intensity of the CD signal at around 350 nm for the four-carboxylic acid rac-H4C was lower than that of rac-H1C. As previously reported[25] and demonstrated above, amino groups are present on the surface of silica nanohelices after APTES modification and it is conceivable that they may interact with carboxy groups of the helicenes through intermolecular interactions such as hydrogen bonding. This suggests that the large number of interaction points between rac-H4C and the ASNH hinders the optimal organization of the helicene molecules required for effective CD induction. In contrast, rac-H1C, with only one point of interaction with the ASNH, allows better molecular organization even after adsorption onto the silica surface.
To verify whether enantioselective adsorption of helicenes occurs on the ASNH, drop-cast films prepared with rac-H1C and rac-H4C were washed with DMF, and the CD signals of the washing solutions and the cast films after washing were measured (Fig. S5a†). The washing solutions from rac-H1C and rac-H4C films showed helicene absorption, but no CD signals were detected (Fig. S5b and c†). In contrast, the cast films (P-S@rac-T1C or H1C and M-S@rac-T1C or H1C) retained their symmetrical CD signals after washing. These results indicate that the CD signals were induced in the racemic mixture of helicenes adsorbed onto the silica nanohelices' surface, rather than arising from enantioselective adsorption.

Supramolecular assembly of helicene molecules on silica surfaces

We then prepared drop-cast films using enantiomers of H1C. Table 3 summarizes the composition ratios of ASNH and helicenes. Fig. S6† shows the DRCD and UV-Vis absorption spectra of drocast films prepared with the P-type H1C enantiomer (P-H1C) and the M-type H1C enantiomer (M-H1C) in the presence or absence of P-S and M-S.
The drop-cast films of P-H1C and M-H1C, with or without ASNH, exhibited mirror-image signals. A positive (negative) CD signal was observed at around 350 nm, while a negative (positive) signal appeared at approximately 250 nm for P-H1C (M-H1C), respectively, regardless of the handedness of the silica nanohelices (Fig. S6†).
The CD spectra were symmetrical for the enantiomeric combinations. The signals were enhanced when the ASNH and helicenes had the same handedness (P-S@P-H1C and M-S@MH1C) and attenuated when they had opposite handedness (P-S@M-H1C and M-S@P-H1C). The drop-cast films of P-H1C and M-H1C alone, without an ASNH, exhibited intermediate CD signals compared to P-S@M-H1C and M-S@M-H1C, or P-S@P-H1C and M-S@P-H1C. These results, along with the CD signals observed for racemic H1C with P-S or M-S, suggest a cooperative effect between the molecular chirality of H1C and the helical supramolecular assemblies of H1C in contact with an ASNH.
The origin of these CD signals observed in the presence of silica nanohelices could be attributed to several possibilities:

Enantioselective adsorption. Selective adsorption of one helicene enantiomer onto silica nanohelices, which depends on the helicity of the latter, exhibits circular dichroism (CD) signals.

Enantioenrichment through helicity conversion. In the case of racemic helicenes, the handedness of the helicenes could change during adsorption, leading to enantioenrichment and CD signals based on the molecular chirality.

Helical supramolecular organization of helicenes in their racemic form around silica nanohelices. The racemic helicenes could form a helical supramolecular organization around the silica nanohelices.

To explore these possibilities, several control experiments were conducted. As described earlier, no enantioselective adsorption was observed, as the supernatants consistently showed no CD signals.

The drop-cast films of P-S or M-S@P-H1C or M-H1C were further washed with DMF, followed by DRCD measurements on the remaining films (Fig. 6). All cast films showed a 60–80% decrease in absorbance after washing. Based on our previous report, the specific surface area of the silica nanohelices was calculated to be approximately 300 $m^2\ g^{-1}$.[38] Using this value, the surface area of silica nanohelices in the cast film (50 µg) was estimated to be 0.015 m^2. When 0.1 µmol (6×10^{16} molecules) of helicenes were initially drop-cast onto the ASNH, and considering a 60–80% reduction through washing, it is estimated that approximately 0.02–0.04 µmol ($12–16 \times 10^{15}$ helicene molecules) remained adsorbed on the 0.015 m^2 silica surface, which corresponds to ca. 1 molecule per nm^2. It is noteworthy that from UV spectra, helicenes entrapped with ASNH can be concluded not to strongly aggregate.

Interestingly, the DRCD spectra changed significantly before and after washing. As shown in Fig. 6a, the CD signal which shows a peak at around 340 nm corresponds to the molecular CD signals of the enantiomers alone (Fig. S6†). This signal was enhanced when the helicenes were paired with an ASNH of the same handedness (P-S@P-H1C and M-S@M-H1C) and suppressed when paired with an ASNH of the opposite handedness (P-S@M-H1C and M-S@P-H1C). After washing, the intensity of this peak was significantly reduced (Fig. 6a). The postwash signals resembled those of the racemic helicenes adsorbed onto an ASNH. This suggests that the peak at 340 nm originates from loosely attached, non-organized helicene molecules, which primarily exhibit molecular CD-based signals (outer layer) (Fig. 6d). As a result, this peak is not observed for racemic helicenes adsorbed onto an ASNH (Fig. 5b). After washing, the CD signals are primarily dominated by the CD contributions of helically assembled helicenes.

Notably, the CD signals of racemic helicenes adsorbed onto an ASNH also changed after washing, exhibiting a blue shift (P-S@rac-H1C and M-S@rac-H1C) (Fig. 6c). The DRCD and UV-Vis absorption spectra of the washed cast films for P-S@P-H1C, P-S@M-H1C, and their combined spectra (P-S@PH1C + P-S@M-H1C), as well as M-S@P-H1C, M-S@M-H1C, and their combined spectra (M-S@P-H1C + M-S@M-H1C), are compared to the spectra of racemic helicenes with an ASNH (Fig. 7a and b). For P-S@P-H1C and M-S@M-H1C, which are combinations of helicenes and ASNHs with the same handedness, symmetric CD signals were observed over the wavelength range of 220–400 nm. In contrast, for P-S@M-H1C and M-S@PH1C, combinations of helicenes and ASNH with opposite handedness, the CD signals were blue-shifted, appearing in the 220–320 nm range. The blueshift in the CD signal may be due to the different states of the helicenes assembled on the ASNH surface. As shown in Fig. 6d, helicenes are adsorbed on the ASNH surface via hydrogen bonding. When helicenes bind to ASNH, the interaction is thought to cause the helicenes to align and form a helical structure. The difference in the orientation of helicenes is thought to be responsible for the difference in the wavelength at which the CD signal appears. The combination of helicenes and the ASNH with opposite handedness indicates that the helicenes are closely orientated, while the combination of helicenes and the ASNH with the same handedness indicates that the helicenes are loosely (randomly) orientated. Due to this difference in helicene orientation, the combination of helicenes and ASNH with opposite handedness is believed to alter the electron density distribution, resulting in an increase in transition energy and a subsequent blue shift in the absorption wavelength. The pink and green lines of Fig. 7b show the addition of the CD spectra of M-H1C and P-H1C on P-S, and M-H1C and P-H1C on M-S, respectively. These calculated curves for P-S@M-H1C + P-S@PH1C (pink line) and M-S@P-H1C + M-S@M-H1C (green line) closely resembled the spectra of the racemic helicene cast films, P-S@rac-H1C (red line) and M-S@rac-H1C (blue line). This confirms that the chirality induced in racemic helicenes on ASNHs originates from two types of helical supramolecular assemblies with different orientations of helicene molecules, as illustrated in the schematic diagram in Fig. 7c.

These P-S and M-S@rac-H1C combinations also exhibited distinct induced circularly polarized luminescence (CPL) signals. Fig. 8 shows the CPL and fluorescence spectra of cast films prepared with various helicenes adsorbed onto ASNHs. Six helicenes were used in this study: rac-T1C, three forms of H1C (racemic, P-type, and M-type), rac-P4C, and rac-H4C. For all the helicenes, mirror-image CPL signals (with g_{lum} values around 10^{-3}) were observed when adsorbed onto the ASNH. rac-T1C, rac-P4C, and rac-H4C showed fluorescence peaks at 500 nm and 550 nm (both for rac-P4C and rac-H4C), with corresponding mirror-image CPL signals that matched the handedness of the silica helices—positive for P-S and negative for M-S (Fig. 8a, c and d). For the H1C cast films, all helicenes (enantiomers P-, M-, and racemic H1C) exhibited fluorescence peaks at 525 nm, and CPL signals were observed at the same wavelength (Fig. 8b).

Interestingly, while the CD signals showed significant differences depending on the diastereomeric combinations of ASNH and helicene handedness, the CPL signals were primarily determined by the handedness of the silica helices. Positive CPL signals were observed when helicenes were adsorbed onto P-S helices, and negative signals were observed with M-S helices. Only slight variations in intensity and peak positions were noted between the different combinations (P-S or M-S paired with P-H1C, M-H1C, or rac-H1C).

Conclusions

Cast films of carboxylated helicenes (rac-T1C, rac-H1C, rac-P4C, rac-H4C, P-H1C, and M-H1C) adsorbed onto the surface of amine-functionalized silica nanohelices were prepared by drop-casting helicene solutions onto silica nanohelices. For all the helicenes, clear induced CD and CPL signals were observed upon contact with the silica helices. No enantioselective adsorption was observed when racemic helicenes were used, suggesting that supramolecular assemblies of enantiomeric helicenes formed on the silica surface in a 1 : 1 (P :M) ratio. Thus, the chiroptical signals were induced solely by the adsorption and subsequent helical organization of helicenes on the silica nanohelices' surface. When enantiomeric helicenes were adsorbed onto the silica helices, the resulting CD spectra showed combined contributions from molecular chirality and chiral supramolecular organization, depending on the handedness of both the helicenes and the silica nanohelices. The combination of silica nanohelices and helicenes handedness reveals that different orientations of helicenes in helical supramolecular assemblies were formed at the silica surface. This orthogonal and hierarchical combination of chiroptical signals from the helicenes and silica nanohelices provides an original approach for developing novel materials with tunable chiroptical properties.

Acknowledgements

We acknowledge the financial support from the JSPS Overseas Research Fellowships of Japan Society for the Promotion of Science, the French National Agency for Research, Région Nouvelle-Aquitaine, and Idex Bordeaux (Research Program GPR LIGHT). The CNRS and the University of Angers are acknowledged for the financial support.

References

1 F. Zhao, J. Zhao, Y. Wang, H. T. Liu, Q. Shang, N. Wang, X. Yin, X. Zheng and P. Chen, Dalton Trans., 2022, 51, 6226.
2 Y. Shen and C. F. Chen, Chem. Rev., 2012, 112, 1463.
3 M. E. S. Moussa, M. Srebro, E. Anger, N. Vanthuyne, C. Roussel, C. Lescop, J. Autschbach and J. Crassous, Chirality, 2013, 25, 455.
4 M. A. Medel, C. M. Cruz, D. Miguel, V. Blanco, S. P. Morcillo and A. G. Campana, Angew. Chem., Int. Ed., 2021, 60, 22051.
5 M. Toya, T. Omine, F. Ishiwari, A. Saeki, H. Ito and K. Itami, J. Am. Chem. Soc., 2023, 145, 11553.
6 M. Gingras, Chem. Soc. Rev., 2013, 42, 968.
7 Y. Nakai, T. Mori, K. Sato and Y. Inoue, J. Phys. Chem. A, 2013, 117, 5082.
8 N. Hafedh, F. Aloui and S. Raouafi, J. Mol. Struct., 2018, 1165, 126.
9 D. C. Harrowven, I. L. Guy and L. Nanson, Angew. Chem., Int. Ed., 2006, 45, 2242.
10 D. Schweinfurth, M. Zalibera, M. Kathan, C. Shen, M. Mazzolini, N. Trapp, J. Crassous, G. Gescheidt and F. Diederich, J. Am. Chem. Soc., 2014, 136, 13045.
11 M. Yamaguchi, H. Okubo and M. Hirama, Chem. Commun., 1996, 1771.
12 P. Rahe, M. Nimmrich, A. Greuling, J. Schutte, I. G. Stara, J. Rybacek, G. Huerta-Angeles, I. Stary, M. Rohlfing and A. Kuhnle, J. Phys. Chem. C, 2010, 114, 1547.
13 M. W. van der Meijden, T. Balandina, O. Ivasenko, S. D. Feyter, K. Wurst and R. M. Kellogg, Chem. – Eur. J., 2016, 22, 14633.
14 M. Samal, J. Rybacek, J. Holec, J. Hanus, J. Vacek, M. Budesinsky, L. Bednarova, P. Fiedler, M. S. Slusna, I. G. Stara and I. Stary, Chem. Commun., 2022, 58, 12732.
15 J. Holec, J. Rybacek, J. Vacek, M. Karras, L. Bednarova, M. Budesinsky, M. Slusna, P. Holy, B. Schmidt, I. G. Stara and I. Stary, Chem. – Eur. J., 2019, 25, 11494.
16 M. Jakubec, S. Hansen Trøøyen, I. Cisarova, J. Sykora and J. Storch, Org. Lett., 2020, 22, 3905.
17 N. Zigon and N. Avarvari, CrystEngComm, 2022, 24, 1942.
18 M. Samal, L. Sturm, M. Banasiewicz, I. Deperasinska, B. Kozankiewicz, O. Morawski, Y. Nagata, P. Dechambenoit, H. Bock, A. Rossel, M. Budesinsky, A. Boudier and A. Jancarik, Chem. Sci., 2024, 15, 9842.
19 A. Robert, G. Naulet, H. Bock, N. Vanthuyne, M. Jean, M. Giorgi, Y. Carissan, C. Aroulanda, A. Scalabre, E. Pouget, F. Durola and Y. Coquerel, Chem. – Eur. J., 2019, 25, 14364.
20 T. Delclos, C. Aime, E. Pouget, A. Brizard, I. Huc, M. H. Delville and R. Oda, Nano Lett., 2008, 8, 1929.
21 A. Scalabre, Y. Okazaki, B. Kuppan, T. Buffeteau, F. Caroleo, G. Magna, D. Monti, R. Paolesse, M. Stefanelli, S. Nlate, E. Pouget, H. Ihara, D. M. Bassani and R. Oda, Chirality, 2021, 33, 494.
22 W. Yospanya, M. Nishijima, Y. Araki, T. Buffeteau, E. Pouget, T. Wada and R. Oda, Chem. Commun., 2020, 56, 10058.
23 P. Pranee, A. Scalabre, C. Labrugere, N. Ryu, A. Yano, N. Hano, D. Talaga, Y. Okazaki, E. Pouget, S. Nlate, S. Bonhommeau, M. Takafuji, T. Wada, H. Ihara, T. Buffeteau, D. M. Bassani and R. Oda, Chem. Commun., 2023, 59, 9762.
24 P. Liu, W. Chen, Y. Okazaki, Y. Battie, L. Brocard, M. Decossas, E. Pouget, P. Muller-Buschbaum, B. Kauffmann, S. Pathan, T. Sagawa and R. Oda, Nano Lett., 2020, 20, 8453.
25 J. Cheng, G. L. Saux, J. Gao, T. Buffeteau, Y. Battie, P. Barois, V. Ponsinet, M. H. Delville, O. Ersen, E. Pouget and R. Oda, ACS Nano, 2017, 11, 3806.
26 A. Scalabre, A. M. Gutierrez-Vilchez, A. Sastre-Santos, F. Fernández-Lázaro, D. M. Bassani and R. Oda, J. Phys. Chem. C, 2020, 124, 23839.
27 M. J. Álvaro-Martins, J. Garcés-Garcés, A. Scalabre, P. Liu, F. Fernández-Lázaro, Á. Sastre-Santos, D. M. Bassani and R. Oda, ChemPhysChem, 2023, 24, e202200573.
28 G. Duroux, L. Robin, P. Liu, E. Dols, M. D. S. L. Mendes, S. Buffière, E. Pardieu, A. Scalabre, T. Buffeteau, S. Nlate, R. Oda, M. S. Raju, M. Atzori, C. Train, G. L. J. A. Rikken, P. Rosa, E. A. Hillard and E. Pouget, Nanoscale, 2023, 15, 12095.
29 M. Jaber, T. Georgelin, H. Bazzi, F. Costa-Torro, J. Lambert, G. Bolbach and G. Clodic, J. Phys. Chem. C, 2014, 118, 25447.
30 J. Bujdak, M. Remko and B. M. Rode, J. Colloid Interface Sci., 2006, 294, 304.
31 K. Ernst, Surf. Sci., 2024, 749, 122569.
32 A. Rieger, C. Sax, T. Bauert, C. Wackerlin and K. Ernst, Chirality, 2018, 30, 369.
33 J. N. James and D. S. Sholl, Curr. Opin. Colloid Interface Sci., 2008, 13, 60.
34 H. Guédouar, B. Ben Hassine and F. Aloui, C. R. Chim., 2019, 22, 310–315.
35 Y. Zhang, J. L. Petersen and K. K. Wang, Tetrahedron, 2008, 64, 1285–1293.
36 L. Sturm, F. Aribot, L. Soliman, H. Bock and F. Durola, Eur. J. Org. Chem., 2022, e202200196.
37 J. Barroso, J. L. Cabellos, S. Pan, F. Murillo, X. Zarate, M. A. Fernandez-Herrera and G. Merino, Chem. Commun., 2017, 54, 188–191.
38 P. Liu, Optically active luminescent nanocrystals complexed with chiral silica nanoribbons, PhD thesis, Université de Bordeaux, Kyoto university, 2021.

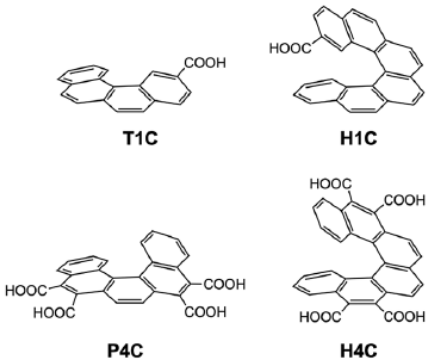

Fig. 1 The chemical structure of helicene derivatives. (a) [4]helicene carboxylic acid (T1C), (b) [6]helicene carboxylic acid (H1C), (c) [5]helicene tetracarboxylic acid (P4C) and (d) [6]helicene tetracarboxylic acid (H4C).

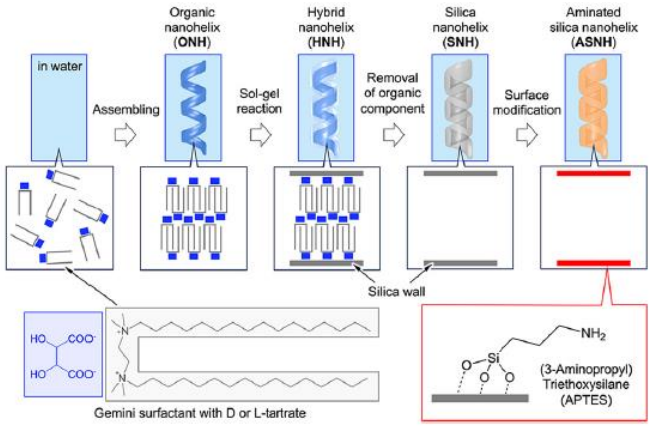

Fig. 2 Schematic illustration of the preparation procedure of aminated silica nanohelices (ASNH).

Table 1 Composition of silica nanohelix and helicene in mixed solutions

Sample name	Silica nanohelix (mg mL^{-1})	Helicenes (mM)
P-$S_{1.0}$@*rac*-$H1C_{0.5}$	1.0	0.5
M-$S_{1.0}$@*rac*-$H1C_{0.5}$	1.0	0.5
P-$S_{1.0}$@*rac*-$H4C_{0.3}$	1.0	0.3
M-$S_{1.0}$@*rac*-$H4C_{0.3}$	1.0	0.3
P-$S_{0.2}$@*rac*-$H4C_{0.3}$	0.2	0.3
M-$S_{0.2}$@*rac*-$H4C_{0.3}$	0.2	0.3

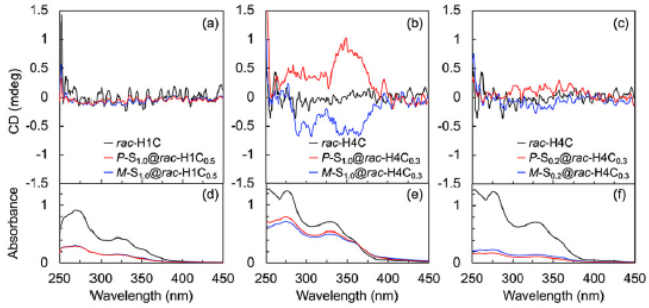

Fig. 3 CD (a–c) and UV-vis absorption (d–f) spectra of supernatant and precipitates of ASNH and helicene mixtures. (a and d) ASNH: 1.0 mg mL^{-1}, *rac*-H1C: 0.5 mM, (b and e) ASNH: 1.0 mg mL^{-1}, *rac*-H4C: 0.3 mM and (c and f) ASNH: 0.2 mg mL^{-1}, *rac*-H4C: 0.3 mM.

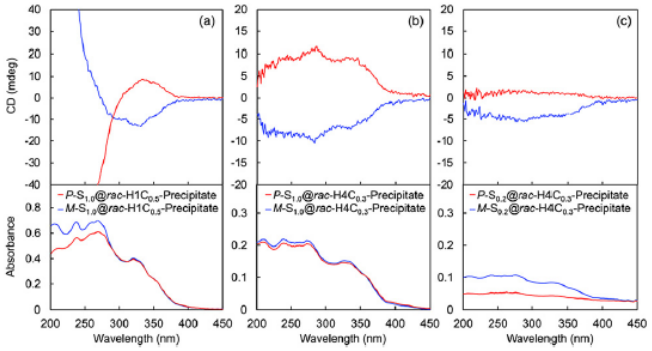

Fig. 4 DRCD and UV-vis absorption spectra of precipitate after drop-casting. (a) *rac*-H1C, (b) and (c) *rac*-H4C.

Table 2 Composition of silica nanohelix and helicene in drop-cast films

		Helicenes	
Sample name	Silica nanohelices (μg cm^{-2})	Name	(μmol)
rac-T1C	—	*rac*-T1C	0.1
P-S@*rac*-T1C	50		
M-S@*rac*-T1C	50		
rac-H1C	—	*rac*-H1C	0.1
P-S@*rac*-H1C	50		
M-S@*rac*-H1C	50		
rac-P4C	—	*rac*-P4C	0.1
P-S@*rac*-P4C	50		
M-S@*rac*-P4C	50		
rac-H4C	—	*rac*-H4C	0.1
P-S@*rac*-H4C	50		
M-S@*rac*-H4C	50		

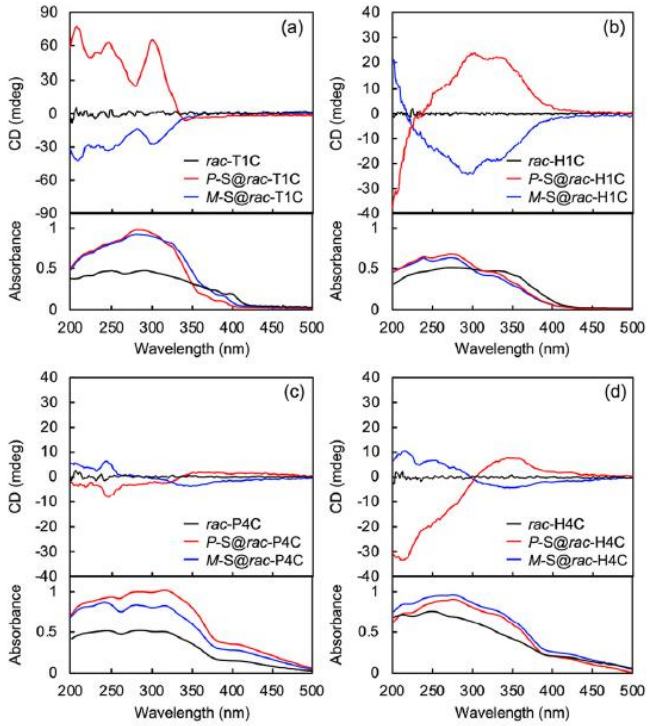

Fig. 5 DRCD and UV-vis absorption spectra of drop-cast films prepared with ASNH and racemic helicene. (a) *rac*-T1C, (b) *rac*-H1C, (c) *rac*-P4C and (d) *rac*-H4C.

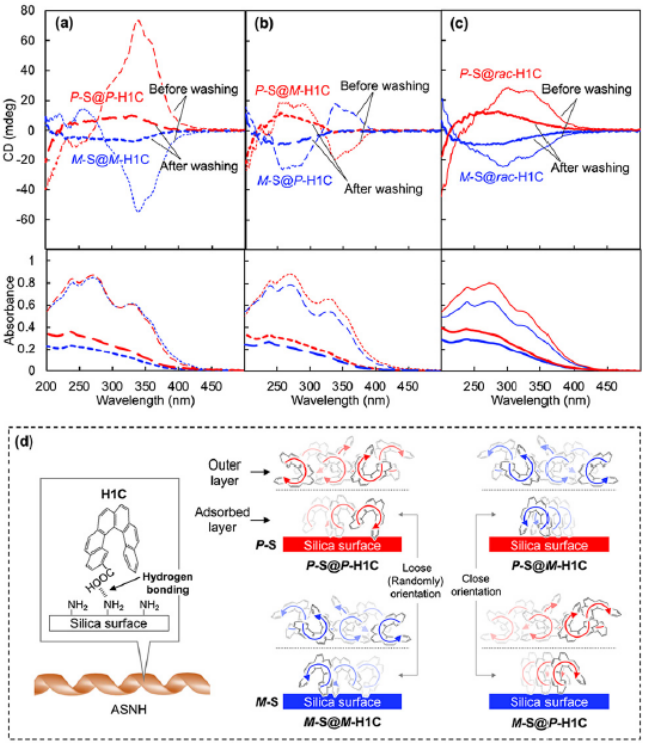

Fig. 6 (a–c) DRCD and UV-vis absorption spectra of drop-cast films prepared with ASNH and enantiomer/racemic H1C before and after washing with DMF. (d) Estimated schematic illustration of helicene molecules on ASNH. (a) *P*-H1C, (b) *M*-H1C and (c) *rac*-H1C.

Table 3 Composition of silica nanohelix and helicene in the drop-cast films

Sample name	Silica nanohelices (μg cm^{-2})	Helicene[a] Name	(μmol)
P-H1C	—	*P*-H1C	0.1
P-S@*P*-H1C	50		
M-S@*P*-H1C	50		
M-H1C	—	*M*-H1C	0.1
P-S@*M*-H1C	50		
M-S@*M*-H1C	50		
rac-H1C	—	*rac*-H1C	0.1
P-S@*rac*-H1C	50		
M-S@*rac*-H1C	50		

[a] *P*-H1C: *P*-type H1C (right-handed), *M*-H1C: *M*-type H1C (left-handed), *rac*-H1C: racemic H1C.

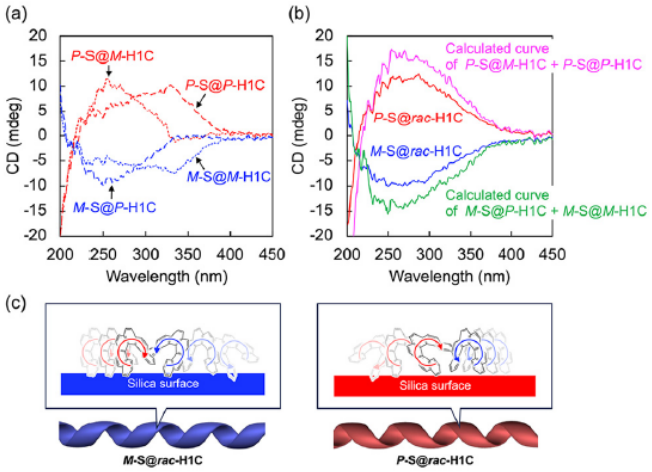

Fig. 7 (a) DRCD spectra of drop-cast films prepared with ASNH and enantiomer H1C after washing with DMF. (b) DRCD spectra of drop-cast films prepared with ASNH and racemic H1C after washing with DMF and calculated curves for the addition of CD spectra of cast films prepared with the two enantiomers (pink and green line). (c) Estimated schematic illustration of racemic helicene molecules on an ASNH.

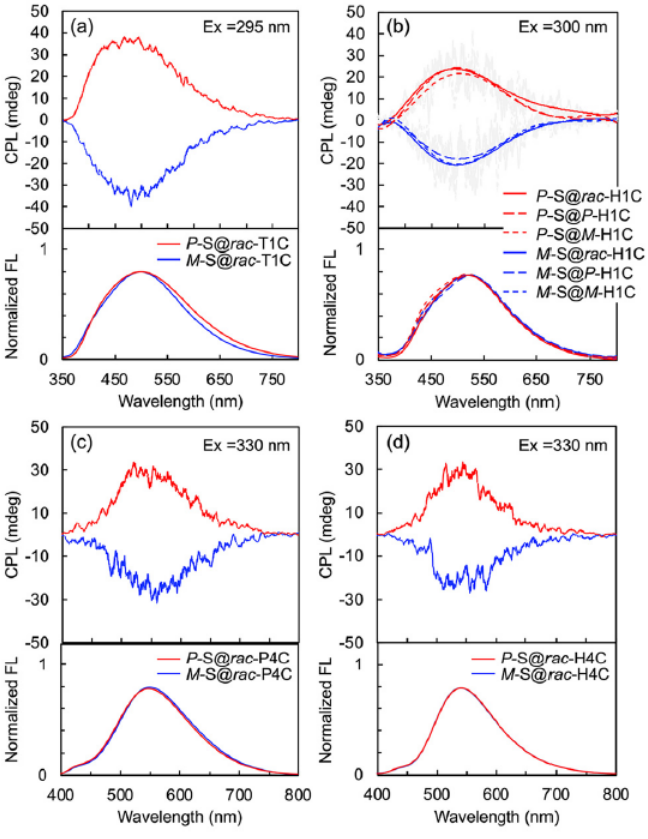

Fig. 8 CPL and fluorescence emission spectra of drop-cast films prepared with ASNHs and various helicenes. (a) *rac*-T1C, (b) *rac*-H1C (c) *rac*-P4C and (d) *rac*-H4C. The excitation wavelengths were 295 nm (a), 300 nm (b) and 330 nm (c and d), respectively.